Journal of Photochemistry and Photobiology A: Chemistry 219 (2011) 1–9

Contents lists available at ScienceDirect

Journal of Photochemistry and Photobiology A: Chemistry

journal homepage: www.elsevier.com/locate/jphotochem

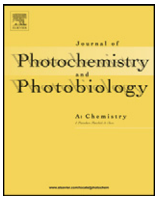

Spectral properties and photobehaviour of 2,5-distyrylfuran derivatives

Serena Ciorba[a], Benedetta Carlotti[a], Irena Škorić[b,*], Marija Šindler-Kulyk[b], Anna Spalletti[a,**]

[a] Dipartimento di Chimica and Centro di Eccellenza Materiali Innovativi Nanostrutturati (CEMIN), Università di Perugia, 06123 Perugia, Italy
[b] Department of Organic Chemistry, Faculty of Chemical Engineering and Technology, University of Zagreb, Marulićev trg 19, 10000 Zagreb, Croatia

ARTICLE INFO

Article history:
Received 22 September 2010
Received in revised form 17 January 2011
Accepted 18 January 2011
Available online 26 January 2011

Keywords:
Distyrylfuran derivatives
Fluorescence
Triplet properties
Charge-transfer states
Synthesis

ABSTRACT

Four novel *trans*,*trans*-2,5-distyrylfuran derivatives (*E*,*E*-X-DStFs, X = Cl, OCH_3, $N(CH_3)_2$, NO_2) have been synthesized and characterized by ^1H and ^{13}C NMR and UV–vis spectroscopy. The photophysical properties of the excited states of these poorly photoreactive compounds have been studied in two solvents of different polarities by stationary and pulsed techniques and also by the help of semiempirical quantum-mechanical calculations. The high fluorescence efficiency of these systems was accompanied by a modest triplet production (that becomes substantial in the nitro-derivative) investigated by nanosecond laser flash photolysis. The solvent effect on the absorption and emission spectra and on the photobehaviour allowed to evidence the presence of charge transfer (CT) excited states in the dimethylamino- and, particularly, in the nitro-derivative.

1. Introduction

On the line of our interest in design, synthesis and study of hetero-polycyclic compounds [1–12] with conjugated bond structure of potential application as fluorescent probes and in optoelectronics, we recently reported the results of a detailed spectral and photophysical study on 2,3- and 2,5-distyrylfuran derivatives [6] pointing to high fluorescence quantum yields and to a similarity of their spectral behaviour to that of *cis*-α,ω-di phenylpolyenes, particularly for what concerns the presence of the *cis* peak [7,8].

Further investigation of asymmetric 2,3-distyryl-benzofuran derivatives with electron-donor or acceptor groups, in para position to a phenyl ring [9,10], was found very interesting particularly for the formation of intra-molecular charge transfer (ICT) states observed in polar solvents.

This paper deals with the synthesis and photobehaviour of *trans*–*trans* asymmetric 2,5-distyrylfuran derivatives (*EE*-2,5-X-DStF) where X is a chloro, methoxy, dimethylamino or nitro groups in para position, as shown in Scheme 1. Measurements of the spectral properties and photobehaviour, carried out in two solvents of different polarities, allowed a complete description of the deactivation pathways of their excited states. Transient spectroscopy with nanosecond resolution was performed to reveal the involvement of the lowest excited triplet state. A fluorosolvatochromism induced by the solvent polarity was found in the case of dimethylamino and nitro derivatives, being particularly strong in the latter.

2. Experimental

2.1. Synthesis

2.1.1. General

The ^1H and ^{13}C NMR spectra were recorded on a Bruker AV-600 Spectrometer at 300 and 600 MHz. All NMR spectra were measured in $CDCl_3$ using tetramethylsilane as reference. UV spectra were measured on a Varian Cary 50 UV/VIS Spectrophotometer. Mass spectra of the novel compounds were obtained on a Varian CP-3800 Gas Chromatograph-Varian Saturn 2200 (GC/MS) system equipped with FactorFour Capillary Column VF-5ms, 30 m × 0,25 mm ID; GC operating conditions for all experiments: column temperature programmed from 110 °C to 300 °C (6 min isothermal) at a rate of 33 °C min^{-1}; carrier gas: helium; flow rate: 1 mL min^{-1}; injector temperature: 300 °C; volume injected: 5 μL. Melting points were obtained using an Original Kofler Mikroheiztzisch apparatus (Reichert, Wien) and are uncorrected. Elemental analyses were carried out on Perkin-Elmer, Series II, CHNS Analyzer 2400. Silica gel (Merck 0.063–0.2 mm) was used for chromatographic purifications. Thin-layer chromatography (TLC) was performed on Merck precoated silica gel 60 F_{254} plates. Solvents were purified by distillation.

Furan-2-carbaldehyde and *p*-dimethylamino-benzaldehyde were obtained from a commercial source (Aldrich). Different triphenylphosphonium salts, benzyl-, *p*-chlorobenzyl-, *p*-

---

* Corresponding author. Tel.: +385 1 4597241; fax: +385 1 4597250.
** Corresponding author. Tel.: +39 75 5855575; fax: +39 75 5855598.
E-mail addresses: iskoric@fkit.hr (I. Škorić), faby@unipg.it (A. Spalletti).

1010-6030/$ – see front matter © 2011 Elsevier B.V. All rights reserved.
doi:10.1016/j.jphotochem.2011.01.009

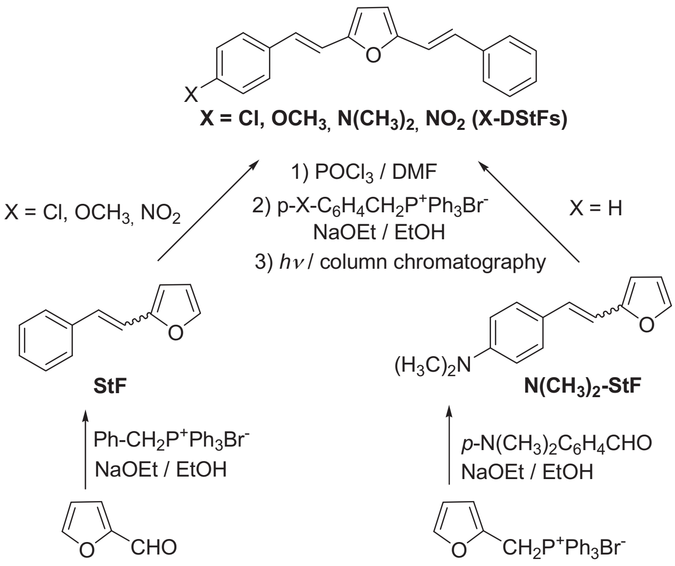

Scheme 1.

methoxybenzyl-, *p*-nitrobenzyl-triphenylphosphonium bromides and 2-furyl-triphenylphosphonium bromide, were synthesized from the corresponding bromides and triphenylphosphine in benzene solution.

2.1.2. *Preparation of trans,trans-2,5-distyrylfuran derivatives (E,E-X-DStFs, X = Cl, OCH₃, N(CH₃)₂, NO₂)*

The investigating compounds are synthesized according to the reaction pathways reported in Scheme 1. To a stirred solution of benzyltriphenylphosphonium bromide (20.0 mmol) and furfural (18.0 mmol) or furfuryltriphenylphosphonium salt (20.0 mmol) and *p*-dimethylaminobenzaldehyde, respectively, in absolute ethanol (100 mL) a solution of sodium ethoxide (0.615 g, 27.0 mmol in 10 mL ethanol) was added dropwise (Scheme 1). Stirring was continued under a stream of nitrogen for one day at RT. After removal of the solvent, the residue was worked up with water and benzene. The benzene extracts were dried and concentrated. The pure *cis*- and *trans*-2-styrylfuran (StF, 81.8%) and *p*-dimethylamino-2-styrylfuran ($N(CH_3)_2$-StF, 77.4%), respectively, were obtained in the first fractions by column chromatography on silica gel using petroleum ether as an eluent and subjected to formylation. Obtained StF (7.4 mmol) and $N(CH_3)_2$-StF (7.4 mmol), respectively (Scheme 1), were dissolved in dimethylformamide (1.71 mL, 22.0 mmol) and after being stirred at ∼11 °C for 20 min, phosphorus oxychloride (1.14 g, 7.4 mmol) was added and the reaction mixture was allowed gradually to warm up to room temperature and stirred for 4 days. The reaction mixture was decomposed by the continuous addition (with cooling) of 10% sodium hydroxide solution and the product was worked up with diethyl ether. The diethyl ether extracts were washed with water. After removal of the solvent, the crude reaction mixtures of 2-formyl-5-styrylfuran and 2-formyl-5-N,N-dimethylaminostyrylfuran, respectively, as mixtures of *cis*- and *trans*-isomers, were used in the next reaction step. To a stirred solution of formyl derivatives (1.4 mmol) and the corresponding phosphonium salts (1.6 mmol), *p*-chlorobenzyl-, *p*-methoxybenzyl-, *p*-nitrobenzyl- and benzyltriphenylphosphonium bromides, respectively, in absolute ethanol (100 mL) a solution of sodium ethoxide (0.05 g, 2.2 mmol in 10 mL ethanol) was added dropwise. Stirring was continued under a stream of nitrogen for one day at RT. After removal of the solvent, the residue was worked up with water and benzene. The benzene extracts were dried and concentrated. The crude reaction mixture was purified and the mixture of four isomers of asymmetric X-DStFs was obtained by column chromatography on silica gel using petroleum ether/ diethyl ether (0–5%) mixture as the eluent. A mixture of isomers in benzene (∼5.5 mM) was purged with argon for 15 min and irradiated at 350 nm in a Rayonet reactor in a pyrex tube. The photochemical isomerization was followed by GC-MS measurements. After 15–30 min the reaction mixture contained 85–95% of the *trans,trans*-isomers of X-DStFs. The solvent was removed *in vacuo* and the oily residue chromatographed on silica gel column using petroleum ether to isolate pure *E,E*-X-DStFs in the last fractions. Characterization data of the new *E,E*-X-DStFs are given below.

2.1.2.1. 2-[2-(4-Chlorophenyl)ethenyl]-5-(2-phenylethenyl)furan (Cl-DStF): overall yield 49%. *E,E*-Cl-DStF: R_f 0.64 (petroleum ether/CH_2Cl_2, 9:1); yellow solid; mp 144 °C; ^{1}H NMR (600 MHz, $CDCl_3$) δ_H 7.50 (d, J = 7.5 Hz, 2H), 7.44 (d, J = 8.2 Hz, 2H), 7.36 (t, J = 7.5 Hz, 2H), 7.32 (d, J = 8.2 Hz, 2H), 7.26 (t, J = 7.5 Hz, 1H), 7.13 (d, J = 16.3 Hz, 1H, H_{et}), 7.07 (d, J = 16.2 Hz, 1H, H_{et}), 6.88 (d, J = 16.2 Hz, 1H, H_{et}), 6.85 (d, J = 16.3 Hz, 1H, H_{et}), 6.40 (d, J = 3.5 Hz, 1H), 6.39 (d, J = 3.5 Hz, 1H); ^{13}C NMR (75 MHz, $CDCl_3$) δ_C 152.72 (s), 152.15 (s), 136.48 (s), 135.10 (s), 132.61 (s), 128.40 (d), 128.28 (d), 127.19 (2d), 127.01 (2d), 126.97 (2d), 125.88 (2d), 125.36 (d), 116.19 (d), 115.63 (d), 111.23 (d), 110.78 (d); MS (EI) m/z (%) 307 (M^+, 100). Anal. Calcd for $C_{20}H_{15}OCl$ (M_r = 306.79): C, 78.30; H, 4.93. Found: C, 78.17; H 5.17.

2.1.2.2. 2-[2-(4-Methoxyphenyl)ethenyl]-5-(2-phenylethenyl)furan (CH_3O-DStF): overall yield 51%. *E,E*-CH_3O-DStF: R_f 0.60 (petroleum ether/CH_2Cl_2, 9:1); yellow-green solid; mp 168 °C; ^{1}H NMR (600 MHz, $CDCl_3$) δ_H 7.49 (d, J = 7.5 Hz, 2H), 7.44 (d, J = 8.4 Hz, 2H), 7.35 (t, J = 7.5 Hz, 2H), 7.24 (t, J = 7.5 Hz, 1H), 7.11 (d, J = 16.2 Hz, 1H, H_{et}), 7.09 (d, J = 16.2 Hz, 1H, H_{et}), 6.90 (d, J = 8.4 Hz, 2H), 6.88 (d, J = 16.2 Hz, 1H, H_{et}), 6.76 (d, J = 16.2 Hz, 1H, H_{et}), 6.38 (d, J = 3.4 Hz, 1H), 6.33 (d, J = 3.4 Hz, 1H), 3.84 (s, 3H, OCH_3); ^{13}C NMR (75 MHz, $CDCl_3$) δ_C 159.35 (s), 153.35 (s), 152.63 (s), 137.15 (s), 129.88 (s), 128.71 (2d), 127.62 (2d), 127.50 (d), 127.01 (d), 126.90 (d), 126.31 (2d), 116.27 (d), 114.31 (d), 114.22 (2d), 111.30 (d), 110.39 (d), 55.35 (q); MS (EI) m/z (%) 302 (M^+, 100), 211 (5), 167 (10), 84 (15). Anal. Calcd for $C_{21}H_{18}O_2$ (M_r = 302.00): C, 83.42; H, 6.00. Found: C, 83.16; H 5.85.

2.1.2.3. 2-[2-(4-Nitrophenyl)ethenyl]-5-(2-phenylethenyl)furan (NO_2-DStF): overall yield 39%. *E,E*-NO_2-DStF: R_f 0.55 (petroleum ether/CH_2Cl_2, 9:1); orange-red solid; mp 139 °C; ^{1}H NMR (600 MHz, $CDCl_3$) δ_H 8.21 (d, J = 8.4 Hz, 2H), 7.60 (d, J = 8.4 Hz, 2H), 7.51 (d, J = 7.6 Hz, 2H), 7.37 (t, J = 7.6 Hz, 2H), 7.24 (t, J = 7.6 Hz, 1H), 7.18 (d, J = 16.2 Hz, 1H, H_{et}), 7.15 (d, J = 16.6 Hz, 1H, H_{et}), 7.02 (d, J = 16.2 Hz, 1H, H_{et}), 6.91 (d, J = 16.6 Hz, 1H, H_{et}), 6.53 (d, J = 3.4 Hz, 1H), 6.44 (d, J = 3.4 Hz, 1H); ^{13}C NMR (75 MHz, $CDCl_3$) δ_C 154.24 (s), 154.97 (s), 143.69 (s), 138.97 (s), 136.73 (s), 128.80 (2d), 128.56 (d), 127.99 (d), 126.56 (2d), 126.50 (2d), 124.39 (d), 124.24 (2d), 120.07 (d), 115.90 (d), 114.03 (d), 111.49 (d); MS (EI) m/z (%) 317 (M^+, 100). Anal. Calcd for $C_{20}H_{15}NO_3$ (M_r = 317.34): C, 75.70; H, 4.76. Found: C, 75.97; H 4.61.

2.1.2.4. 2-[2-(4-Dimethylaminophenyl)ethenyl]-5-(2-phenylethenyl)furan [$(CH_3)_2N$-DStF]: overall yield 44%. *E,E*-$(CH_3)_2N$-DStF: R_f 0.52 (petroleum ether/CH_2Cl_2, 9:1); green-yellow solid; mp 188–190 °C; ^{1}H NMR (300 MHz, $CDCl_3$) δ_H 7.47 (d, J = 7.3 Hz, 2H), 7.38 (d, J = 8.7 Hz, 2H), 7.33 (t, J = 7.3 Hz, 2H), 7.21 (t, J = 7.3 Hz, 1H), 7.08 (d, J = 15.9 Hz, 1H), 7.06 (d, J = 16.3 Hz, 1H), 6.85 (d, J = 16.3 Hz, 1H), 6.69 (d, J = 15.9 Hz, 1H), 6.68 (d, J = 8.7 Hz, 2H), 6.34 (d, J = 3.4 Hz, 1H), 6.27 (d, J = 3.4 Hz, 1H), 2.96 (s, 6H, CH_3); ^{13}C NMR (75 MHz, $CDCl_3$) δ_C 154.10 (s), 152.33 (s), 150.23 (s), 137.43 (s), 128.71 (2d), 127.93 (d), 127.67 (2d), 127.42 (d), 126.40 (d), 126.35 (2d), 125.54 (s), 116.48 (d), 112.51 (2d), 112.32 (d), 111.41 (d), 109.46 (d), 40.40 (2q); MS (EI) m/z (%) 315 (M^+, 100). Anal. Calcd for $C_{22}H_{21}NO$ ($M_r = 315.41$): C, 83.78; H, 6.71. Found: C, 83.92; H 6.44.

Further purification of investigating *E,E*-X-DStFs was performed by semi-preparative HPLC equipped by Prontosil C30 (5μ, 250 mm × 20 mm) column and UV detector.

2.2. Spectral, photochemical and photophysical experiments

The irradiation of deaerated (by bubbling pure nitrogen) solutions of X-DStFs in cyclohexane (CH) and acetonitrile (AcN) was also performed in mild conditions (concentration $\cong 10^{-4}$ M, low dose of the monochromatic excitation light). The excitation wavelength, corresponding to the maximum of the first band of the absorption spectrum, was isolated from a 150 W high pressure Xenon lamp by a monochromator. The photoreaction was monitored by HPLC Waters apparatus equipped with analytical Prontosil 200-3-C30 (3μ, 250 mm × 4 mm) column and UV diode-array detector using water–acetonitrile mixtures as the eluent.

A Perkin-Elmer Lambda 800 spectrophotometer was used for the absorption measurements. The experimental oscillator strength was derived by $f = (4.39 \times 10^{-9}/n) \int \varepsilon(\bar{\nu})\,d\bar{\nu}$ [14], considering the refraction index $n \cong 1$.

The fluorescence spectra were measured by a Spex Fluorolog-2 F112AI spectrofluorimeter. Dilute solutions (absorbance less than 0.1 at the excitation wavelength, λ_{exc}) were used for fluorimetric measurements. 9,10-diphenylanthracene in de-aerated CH was used as fluorimetric standard ($\phi_F = 0.90$) [15]. Fluorescence lifetimes were measured by an Edinburgh Instrument 199S spectrofluorimeter, using the single photon counting method.

All measurements were performed in CH and AcN at room temperature.

The triplet state was investigated in CH and AcN by a nanosecond laser flash photolysis setup previously described (Nd:YAG Continuum, Surelite II, third harmonics, $\lambda_{exc} = 355$ nm, pulse width ca. 7 ns and energy ≤ 1 mJ pulse^{-1}) [16,17]. First-order kinetics were observed for the decay of the lowest triplet state (T–T annihilation was prevented by the low excitation energy). The transient lifetimes (τ_T) were measured at an absorbance of ca. 0.2. The transient spectra were obtained by monitoring the change of absorbance over the 300–800 nm range and averaging at least 10 decays at each wavelength. The experimental setup was calibrated by an optically matched solution of benzophenone in AcN ($\phi_T = 1$ and $\Delta\varepsilon_T = 6500$ M^{-1} cm^{-1} at the corresponding absorption maximum) [18]. Triplet–triplet molar absorption coefficients (ε_T), and then triplet formation yields (ϕ_T), were determined by energy transfer from benzophenone in AcN and from di-(2-thienyl)ketone in CH ($\Delta\varepsilon_T = 5200$ M^{-1} cm^{-1} at 630 nm, the corresponding absorption maximum). In fact, radicals were produced upon irradiation in the polar AcN and the triplet molar absorption coefficient needed to be measured in CH. Since di-(2-thienyl)ketone has a low bimolecular rate constant for hydrogen abstraction [19], it was used to fully characterize the triplet state in CH [20]. The triplet molar absorption coefficient of di-(2-thienyl)ketone ($\Delta\varepsilon_T = 5000$ and 5200 M^{-1} cm^{-1} at λ_{max} in AcN and CH, respectively) was estimated by energy transfer from benzophenone in AcN or to anthracene in CH ($\Delta\varepsilon_T = 52500$ M^{-1} cm^{-1} at 423 nm) [18]. The quenching constants of the transients by molecular oxygen were evaluated by the slope of the linear plots of transient lifetime vs. different oxygen concentrations. Absorption spectra were recorded with a Perkin-Elmer Lambda 800 spectrophotometer before and after the transient absorption measurements to check for photodegradation. To minimize interference by the photoproducts formed in the course of the measurements, the deoxygenated solutions containing the investigated compounds in CH and AcN were flowed through the quartz cell using a continuous-flow system.

The measurements were performed at room temperature and in de-aerated solutions by purging with nitrogen. The parameters reported in the tables are averages of at least three independent measurements with mean deviation of ca. 10% (about 15% for ε_T and ϕ_T).

2.3. Theoretical calculations

The quantum-mechanical calculations were carried out using the HyperChem computational package (version 7.5): total energies and dipole moments were obtained for geometries optimized by HF ab initio (3-21-G level) method. The computed transition energies and oscillator strengths were obtained by ZINDO/S at the optimized geometries, the configuration interaction including 1600 (40 × 40) single excited configurations.

3. Results and discussion

3.1. Synthesis

The investigating compounds, *trans,trans*-2,5-distyrylfuran derivatives (X-DStFs) (X = Cl, OCH_3, $N(CH_3)_2$, NO_2), were prepared in several steps by two Wittig reactions and Vilsmeier formylation (Scheme 1). In the first step 2-styrylfuran (StF) and *p*-dimethylamino-2-styrylfuran ($N(CH_3)_2$-StF) were prepared by Wittig reaction as described for other styrylfurans [13], from benzyltriphenylphosphonium bromide and freshly distilled furan-2-carbaldehyde or from *p*-dimethylamino-benzaldehyde and 2-furyltriphenylphosphonium bromide, respectively. Obtained StF and $N(CH_3)_2$-StF were formylated and subjected to the Wittig reaction with corresponding triphenylphosphonium salts. All X-DStFs were obtained in good overall yield (39–51%) as the mixtures of four isomers, predominantly *trans,trans*-X-DStFs. Pure *trans,trans*-isomers were isolated by column chromatography of the isomer mixtures after their short irradiation.

3.2. Spectral properties

The absorption and emission spectra of the EE isomer of the investigated compounds in two solvents are shown in Fig. 1 and the spectral parameters are collected in Table 1.

The first absorption band, assigned to an allowed transition of ππ* nature, is rather strong and shows an only partially resolved vibrational structure (with the exception of the nitro-derivative in CH). The second strong transition (around 270–300 nm, less intense than the first one and little structured) is assigned to the *cis* peak, in analogy with the spectral behaviour reported for the unsubstituted 2,5-distyrylfuran [6] and hetero-analogues [7,8]. In such molecules the presence of the *cis* peak is due to the specific (*s-cis* type) C═C–C═C arrangement of the central furan or pentatomic heteroaryl ring. Such structural origin of the *cis* peak is different from that, well known, found for arylpolyenes and similar molecules of biological interest (carotenoids and retinals) [21]. In fact, in the latter, the appearance of the *cis* peak is related to the presence of double bond in *cis* configuration that implies a non-linear geometry of low symmetry if compared to the corresponding all-*trans* isomers. In a previous work [7] the similarity of the absorption spectra of 2,5-distyryl(hetero)arenes with that of 3-*cis*-α,ω-diphenyloctatetraene [21] was explained by a similar electronic and molecular structure, due to the scarce aromaticity of the pentatomic central ring.

The presence of the $N(CH_3)_2$ and NO_2 groups shifts the absorption by 20 and 40 nm, respectively, towards the red.

The fluorescence spectra appear to be more structured, at least in non-polar solvent, with a vibronic progression of ca. 1400 cm^{-1}. The polar solvent does not affect too much the absorption and

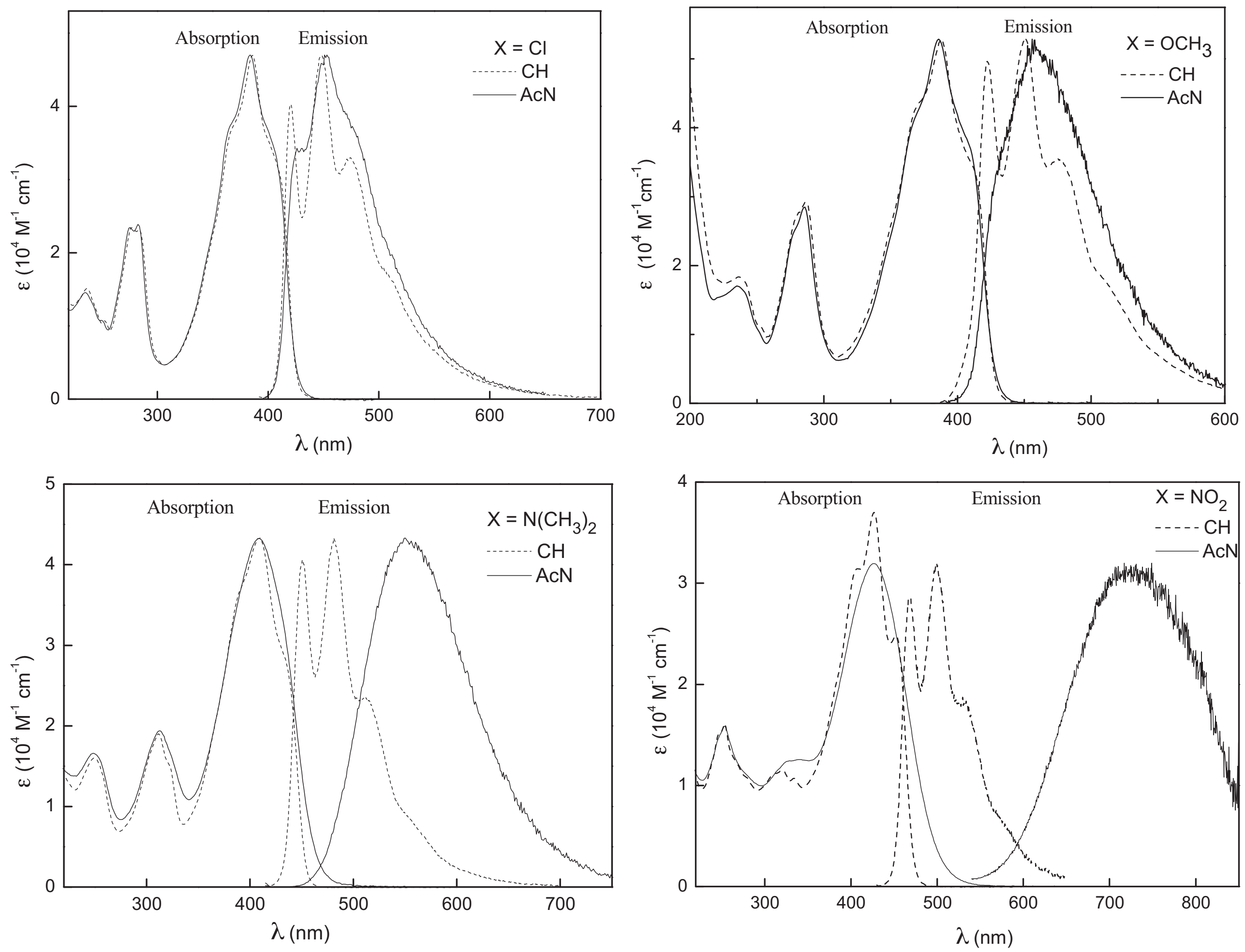

Fig. 1. UV–vis absorption coefficients and fluorescence emission spectra of X-DStFs in CH (dash) and AcN (solid). For X = Cl and OCH_3 the absorption spectra in CH are normalized to those in AcN.

Table 1
Spectral behaviour of the X-DStFs in two solvents at room temperature.[a]

X	Solvent	λ_{abs}^{max} (nm)	$\Delta\tilde{\nu}_{abs}$ (cm^{-1})	λ_{F}^{max} (nm)	$\Delta\tilde{\nu}_{F}$ (cm^{-1})	$\Delta\tilde{\nu}_{S,max}$ (cm^{-1})	$\Delta\tilde{\nu}_{S,00}$ (cm^{-1})
Cl	CH	367^{sh}, $\underline{386}$, 408^{sh}	1370	421, $\underline{448}$, 474	1330	3590	760
	AcN	365^{sh}, $\underline{384}$, 405^{sh}	1350	428, $\underline{453}$, 480	1270	3970	1330
OCH_3	CH	368^{sh}, $\underline{388}$, 410^{sh}	1390	422.5, $\underline{450}$, 477	1450	3550	720
	AcN	367^{sh}, $\underline{386}$, 407^{sh}	1340	431^{sh}, $\underline{459}$	1420	4120	1370
$N(CH_3)_2$	CH	312, 322^{sh}, 387, $\underline{410}$, 436^{sh}	1500	450.5, $\underline{481}$, 515, 555^{sh}	1400	3600	740
	AcN	313, $\underline{408}$		553		6400	
NO_2	CH	405^{sh}, $\underline{427}$, 453	1340	468, $\underline{499.5}$, 535	1340	3400	710
	AcN	428		730		9670	

[a] The underlined wavelengths refer to the maxima; sh means shoulder; $\Delta\tilde{\nu}_{S,00}$ is the difference between the 0,0 transition in absorption and emission.

emission spectra of the first two compounds (that remain in the same region, the fluorescence spectrum loosing its structure) while causes a marked red shift of the fluorescence spectrum for the $N(CH_3)_2$- and NO_2-derivative (by ca. 70 and 230 nm, respectively) that leads to an increased Stokes shift ($\Delta\tilde{\nu}_{S,max}$) in AcN (Table 1). This behaviour points to the presence of an intramolecular charge-transfer (ICT) state in these two compounds that is stabilized in the polar solvent.

3.3. *Quantum-mechanical calculations*

These compounds can exist, in principle, as a mixture of different rotamers that originate from free rotation around the quasi-single bonds between the aromatic groups and the double bonds (see Scheme 2).

However, the calculated total energy values (Table 2) resulted significantly different for the elongated, compressed and semi-compressed conformers indicating that only the most stable compressed rotamer is abundant in solution at room temperature, in agreement with the absence of a significant excitation and emission wavelength effect on the emission and excitation spectra, respectively, and with the mono-exponential decays (see below).

The calculated spectra are in good agreement with the experimental ones (see Table 2). A high oscillator strength ($f \cong 1$) was calculated for the first transition pointing to an allowed character as also indicated by the high k_F values (see Section 3.5). As a mat-

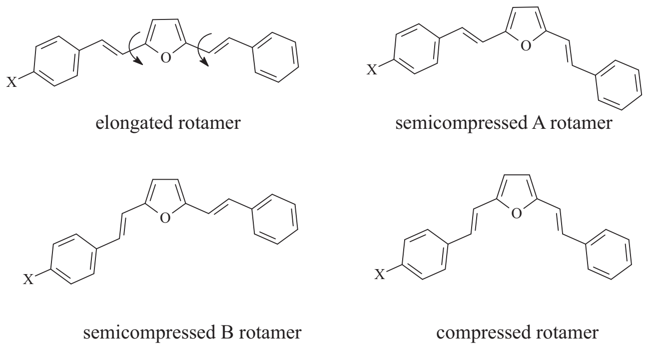

Scheme 2.

ter of fact for NO_2-DStF the theoretical calculations predicted the presence of a lowest forbidden state around 500 nm (as in the case of other nitro-derivatives) [12]. This behaviour can be understood taking into account the solvent effect on the state order which could be inverted going from gas-phase to solution.

The calculated dipole moment of S_1 (μ^*) was found larger than that of S_0 for all the investigated compounds. The photoexcitation produces an increase of μ particularly large in the case of the nitro-derivative (see Table 2). Moreover, it has to be considered that the calculated μ^* refers to a F.C. excited single state because no optimization of the S_1 geometry was performed.

3.4. Photoreactivity

The photoisomerization quantum yields measured under irradiation of X-DStFs in AcN are collected in Table 3. The EE isomers of these asymmetric compounds in non polar solvent (CH) are photostable, the exception being the nitro-derivative that produced a small quantity of a geometrical isomer Y (the second peak in the HPLC chromatogram, $\phi_{EE\rightarrow Y} = 0.030$), that, isolated and irradiated, photoconverted back to EE with a good yield ($\phi_{Y\rightarrow EE} = 0.27$). On the contrary, the nitro-derivative resulted very stable in AcN where the other X-DStFs showed photoisomerization towards the two *cis–trans* stereoisomers (Y and K) with quite different yields. The tentative assignment of the structure of the two photoproducts to ZE and EZ isomers (with the *cis* double bond adjacent to the para-substituted and unsubstituted phenyl ring, respectively, see Scheme 3) was made on the basis of the calculated absorption spectra.

Table 3
Photoisomerization quantum yields under irradiation of the EE isomer of X-DStFs in AcN at room temperature.

X	$\Phi_{EE\rightarrow Y}$	$\Phi_{EE\rightarrow K}$
Cl	0.098	~0.007
OCH_3	0.004	0.027
$N(CH_3)_2$	0.12	–
NO_2	–	–

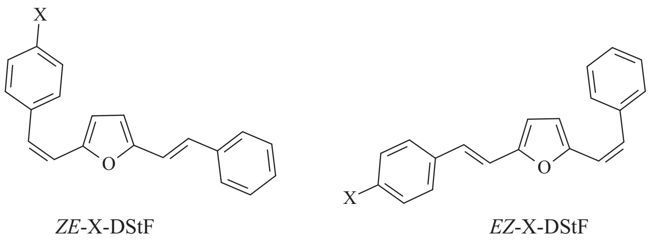

Scheme 3.

In the case of $N(CH_3)_2$- and NO_2-DStF the absorption spectra of the two photoproducts displayed different intensities of the two main bands making possible the structural assignment of the two compounds with different eluation times through the comparison between experimental and calculated spectra. This procedure, shown in Figs. 2 and 3, led to the assignment of the photoproduct Y (second peak) to ZE and K (third peak) to EZ isomer.

In the case of the Cl and OCH_3 derivatives, where the absorption spectra of the two photoproducts are not so different (Fig. 4), the assignment was made by analogy.

Therefore, these asymmetric compounds show a preferential photoisomerization of the double bond adjacent to the substituted benzene in agreement with a localization of the excitation

Table 2
Calculated spectral properties (transition wavelength, λ, and oscillator strength, f), total energy (E_{tot}) and dipole moment (μ) for the rotamers of the investigated X-DStFs. The experimental absorption maximum (λ_{exp}) and oscillator strength (f_{exp}) are reported for comparison.

X	Conformer	μ (D)	μ^* (D)	E_{tot} (kcal/mol)	λ (nm)	f		λ_{exp} (nm)	f_{exp}
Cl	Elongated	3.65	4.77	−811702.063	380	1.55	S_1		
					298	0.13	S_2		
	Semicomp(A)	3.32	4.93	−811704.500	380	1.26	S_1		
					296	0.39	S_2		
	Semicomp(B)	3.76	4.73	−811704.563	382	1.30	S_1		
					298	0.35	S_2		
	Compressed	3.44	4.76	−811707.000	381	0.90	S_1	384	0.94
					295	0.61	S_2	283	0.41
OCH_3	Elongated	2.43	3.63	−596176.688	378	1.64	S_1		
					297	0.14	S_2		
	Compressed	2.00	3.55	−596181.500	383	0.96	S_1	386	0.94
					296	0.57	S_2	286	0.42
$N(CH_3)_2$	Elongated	3.02	3.86	−608157.500	382	1.71	S_1		
					302	0.12	S_2		
	Compressed	2.88	3.34	−608162.438	386	1.01	S_1	409	0.90
					298	0.74	S_3	313	0.42
NO_2	Elongated	7.31	20.37	−652050.188	500	0.000	S_1		
					430	1.33	S_3		
					348	0.41	S_4		
	Compressed	7.01	19.51	−652055.188	500	0.000	S_1		
					435	0.95	S_3	427	0.73
					352	0.30	S_4	330	0.23

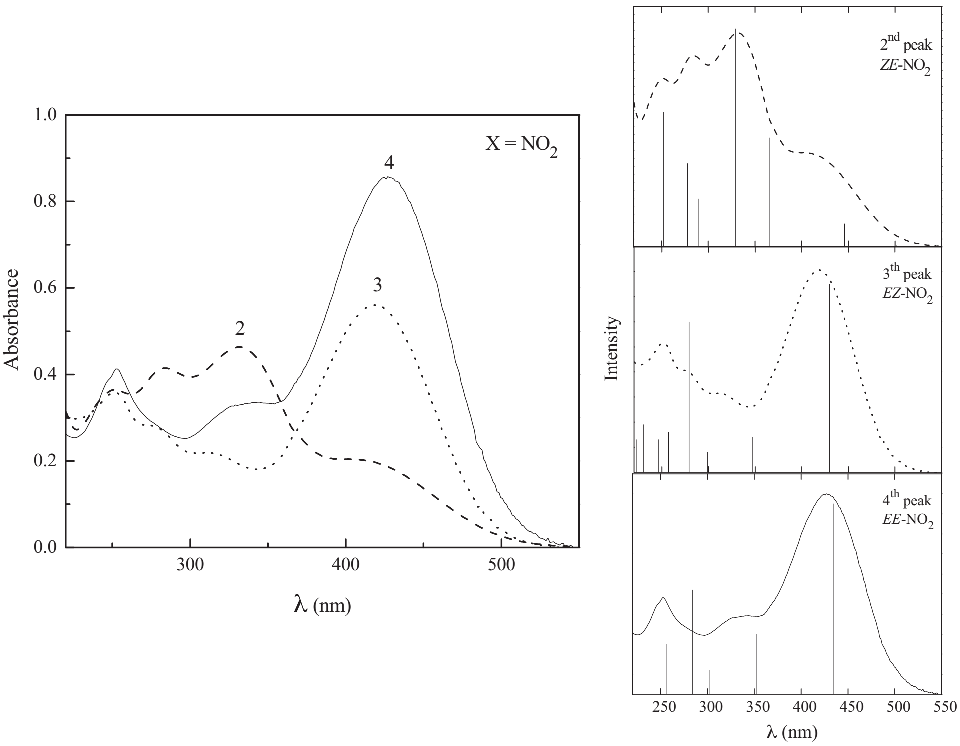

Fig. 2. Absorption spectra of *EE*-NO_2-DStF (4th peak, solid line) and the two photoproducts (2nd and 3rd peak, dash and dot, respectively) produced by irradiation of EE, as obtained by diode-array HPLC analysis. The calculated transitions are also reported.

energy on this moiety (with the exception of methoxy-derivative where the very low reactivity seems to be inverted), as evidenced in the clear case of *EE*-NO_2-DStF by the calculated highest occupied and lowest unoccupied molecular orbitals (HOMO and LUMO, respectively), involved in the main UV–vis transition (Fig. 5).

3.5. Photophysical behaviour

The measured fluorescence quantum yield (ϕ_F) and lifetime (τ_F) of the investigated compounds in non-polar solvent, reported in Table 4, indicate that these compounds are very good fluorophores (little smaller values were found for ϕ_F and τ_F in the case of NO_2-

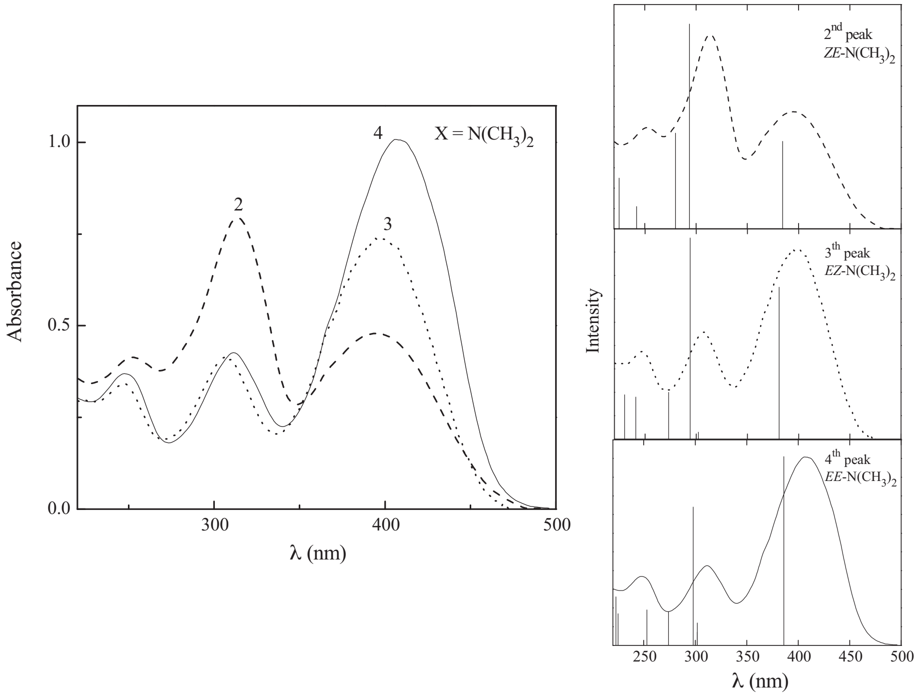

Fig. 3. Absorption spectra of *EE*-$N(CH_3)_2$-DStF (4th peak, solid line) and the two photoproducts (2nd and 3rd peak, dash and dot, respectively) produced by irradiation of EE, as obtained by diode-array HPLC analysis. The calculated transitions are also reported.

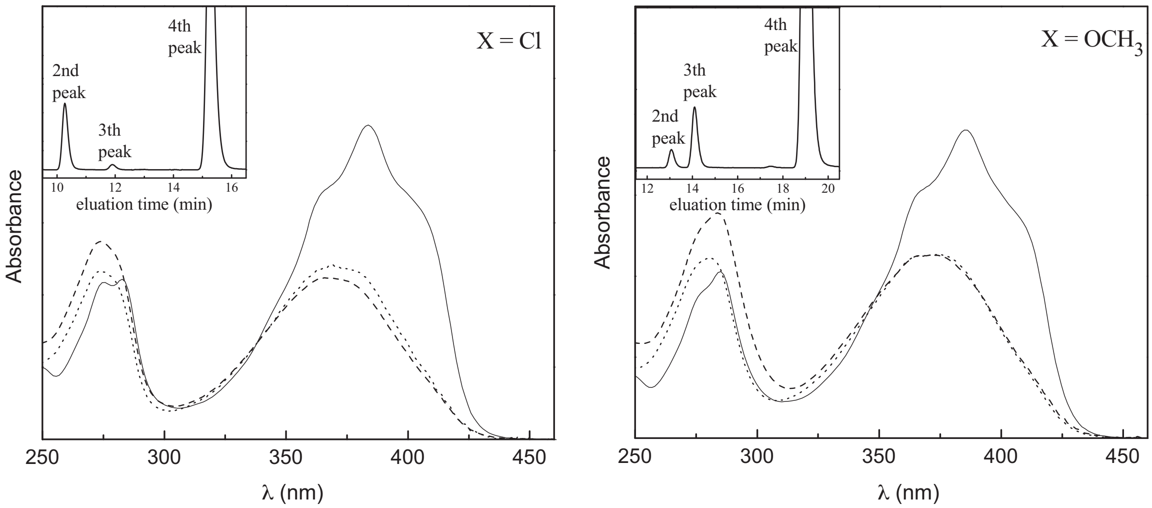

Fig. 4. Absorption spectra of the EE isomers (solid line) of X-DStFs and their photoproducts (2nd peak dashed and 3rd peak dotted line) in water/AcN mixture (10/90, v/v). Insets show the HPLC chromatograms performed after irradiation.

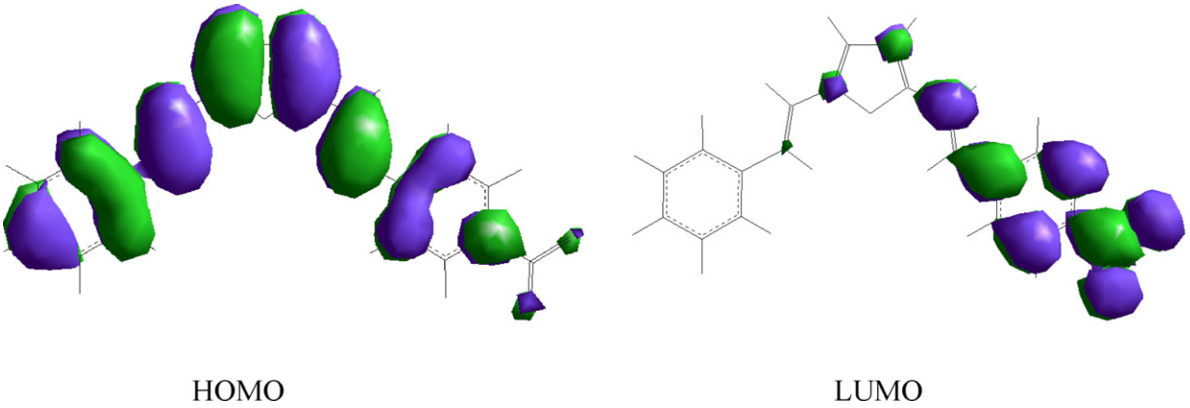

Fig. 5. Molecular orbitals of *EE*-NO$_2$-DStF as derived by ZINDO/S method. The HOMO–LUMO configuration contributes to the main electronic transition with the highest coefficient (0.556).

DStF) that emit through an allowed transition ($k_F \cong 2$–$4 \times 10^8\ s^{-1}$).

The polar solvent affects only slightly the emissive properties of the X-DStFs with the exception of the nitro derivative whose ϕ_F and τ_F decreased more than one order of magnitude on passing from CH to AcN, the τ_F value breaking down under the detectable limit of our experimental setup (~0.5 ns).

A parallel study of the triplet state of the investigated compounds and of the analogous unsubstituted one in the two solvents was very useful to understand the deactivation mechanism of their excited states.

The transient absorption spectra measured by nanosecond flash photolysis under irradiation of Cl- and N(CH$_3$)$_2$-DStF at 355 nm, are reported in Figs. 6 and 7, as an example, together with the decay kinetics recorded at the absorption maximum. The related parameters for all the investigated compounds in two solvents are collected in Table 5.

The spectra exhibit a band of positive absorption in the visible spectral region, which resulted red shifted and broadened for the N(CH$_3$)$_2$- and NO$_2$-derivative with respect to those of OCH$_3$- and Cl-DStF transients in CH. At shorter wavelengths, in the region of the $S_0 \rightarrow S_n$ absorption spectrum, a negative ΔA signal was recorded due to the ground state depopulation (bleaching). The observed transients are assigned to the triplet state because they are efficiently quenched by oxygen ($k_{ox} \cong 1$–$4 \times 10^9\ M^{-1}\ s^{-1}$) and

Table 4

Fluorimetric parameters[a] for the X-DStFs in deaerated CH and AcN at room temperature.

X	Solvent	Φ_F	τ_F (ns)	τ_F/τ_F^a	k_F ($10^8\ s^{-1}$)
Cl	CH	0.81	3.7	1.1	2.2
	AcN	0.63	2.9	1.1	2.2
OCH$_3$	CH	0.82	3.1	1.1	2.6
	AcN	0.79	2.7	1.2	2.9
N(CH$_3$)$_2$	CH	0.83	2.2	1.1	3.8
	AcN	0.70	2.4	1.1	2.9
NO$_2$	CH	0.54	1.6	1.0	3.4
	AcN	0.023	<0.5		>0.5

[a] The a superscript means aerated.

Table 5
Properties of the transients of the *EE*-X-DStFs detected in CH and AcN at room temperature by using nanosecond-resolved laser flash photolysis (λ_{exc} = 355 nm).

X	Solvent	λ_{abs}^{min}, λ_{abs}^{max} (nm)[a,b]	τ_T (μs)[b]	ε_T (M^{-1} cm^{-1})	ϕ_T	k_{ox} (10^9 M^{-1} s^{-1})[b]	Transient
H[c]	CH	390(−), 490(+)	45	19,400	0.13	3.0	T_1
	AcN	380(−),490(+), *580(+)*	37, *62*		0.098	3.0, *0.002*	T_1, $R^{\bullet+}$
Cl	CH	370(−), 490(+)	70	23,800	0.063	2.7	T_1
	AcN	380(−), 490(+), *580(+)*	37, *62*		0.055	*0.004*	T_1, $R^{\bullet+}$
OCH_3	CH	370(−), 500(+)	31	21,000	0.12	1.4	T_1
	AcN	390(−), 510(+), *620(+)*	33, *100*		0.081	*0.0064*	T_1, $R^{\bullet+}$
$N(CH_3)_2$	CH	400(−), 580(+)	74	25,100	0.076	3.2	T_1
	AcN	410(−), *640(+)*	*71*		<0.064	*0.002*	$R^{\bullet+}$
NO_2	CH	430(−), 530(+)	55	27,800	0.65	3.8	T_1
	AcN	430(−), *580(+)*	*40*		<0.013	*0.02*	$R^{\bullet+}$

[a] − means negative signal associated to ground state bleaching, + means positive signal of transient absorption.

[b] The τ_T values and corresponding k_{ox} and λ values in italics refer to the radical cations.

[c] From Ref. [23].

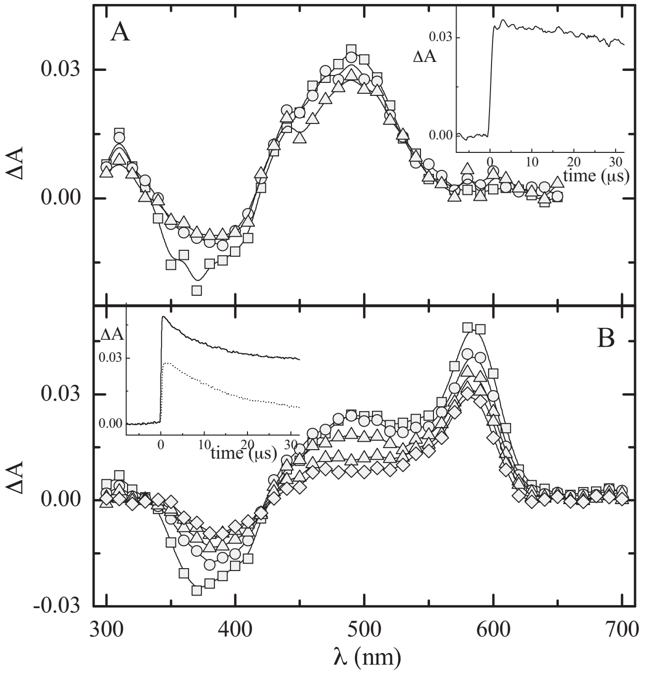

Fig. 6. Transient absorption spectra of *EE*-Cl-DStFs (A) in CH recorded at 0.64 (□), 15.5 (○) and 30.9 (△) μs and (B) in AcN recorded at 0.4 (□), 4.7 (○), 10 (△), 18.9 (▽) and 29.9 (◇) μs after the laser pulse (λ_{exc} = 355 nm). Insets: decay kinetics recorded at 500 nm (A) and 490 and 580 nm (B).

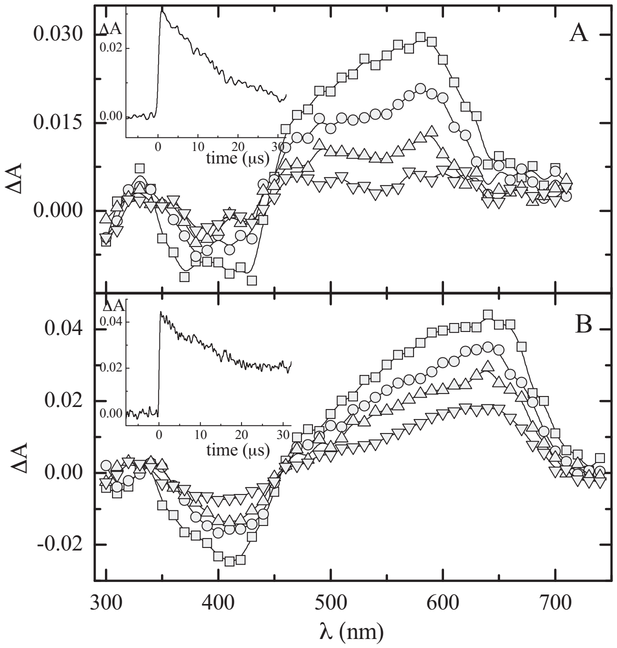

Fig. 7. Transient absorption spectra of *EE*-$N(CH_3)_2$-DStFs (A) in CH, recorded at 1.1 (□), 8.1 (○), 15.8 (△) and 27.5 (▽) μs and (B) in AcN, recorded at 0.4 (□), 5.9 (○), 13.4 (△) and 31.1 (▽) μs after the laser pulse (λ_{exc} = 355 nm). Insets: decay kinetics recorded at 580 nm (A) and 640 nm (B).

produced in sensitized experiments by a triplet energy donor [di-(2-thienyl)ketone].

The absorption band assigned to the triplet resulted generally shifted to the red on going from CH to AcN. Moreover, a second transient absorption peak around 600 nm, not affected by oxygen and characterized by a slightly different decay time, was detected for DStF and its Cl- and OCH_3-derivatives in AcN. Also the broad absorption signals recorded for $N(CH_3)_2$- and NO_2-DStF were not significantly quenched in aerated AcN solution. These experimental results revealed that, together with the triplet, another transient, probably the radical cation ($R^{\bullet+}$) formed by photoionization from excited singlet states, was produced within the laser pulse in polar solvent, as previously found for other distyrylbenzene like molecules [22].

As expected, the ISC is not an important decay channel of S_1 in the case of the unsubstituted DStF and its Cl, OCH_3 and $N(CH_3)_2$ derivatives (ϕ_T around 10% or less), while a substantial production of triplet was found for the nitro-derivative in non-polar solvent (see Table 5), where the substituent induces a substantial increase of ISC [7,12,24]. In the polar solvent the triplet yield was found to decrease also in the case of NO_2-DStF. This fact, together with the strong reduction of ϕ_F and the absence of photoisomerization in AcN, points to the opening of a deactivation pathway that strongly competes with the relaxation processes of S_1. The large bathochromic shift of the fluorescence spectrum of NO_2-DStF in AcN suggests that internal conversion (IC) is the main deactivation channel considering the small S_1–S_0 energy gap. This behaviour is in agreement with the τ_F value in AcN that was estimated smaller than 0.5 ns.

4. Conclusions

The main results of this study can be summarized as:

- The substitution of a H atom in the 2,5-distyrylfuran with a group (X) that makes asymmetric its structure, does not change the spectral behaviour when X = Cl or OCH_3, but causes a positive fluorosolvatochromism due to the introduction of ICT states, in the case of the $N(CH_3)_2$-derivative and particularly when $X = NO_2$ (a strong electron-acceptor) probably because of the π excessive character of the furan central ring.

- The absence of wavelength effects on the excitation and emission spectra and the monoexponential decay point to the presence of a largely prevailing species in solution, the compressed conformer, as confirmed by quantum-mechanical calculations.
- A second band around 280 nm, assigned to the *cis* peak, was evidenced in the absorption spectrum of X-DStFs, as in the case of the unsubstituted compound, pointing to a structure similar to that of diphenyloctatetraene with central double bonds in *cis* configuration, due to the scarcely aromatic character of the furan ring.
- As for 2,5-DStF, the octatetraene-type structure is also related to the very low reactivity of the studied compounds in favour of a prevalent deactivation through fluorescence, with the exception of the nitro-derivative where an ISC pathway becomes competitive with the radiative one in non polar solvents.
- The polar solvent slightly affects the photobehaviour of *EE*-X-DStFs reducing a little the fluorescence quantum yields in favour of a modest selective photoisomerization towards the ZE isomer. The noticeable exception is the nitro-derivative where both the emission and ISC yields are drastically reduced in favour of IC due to a preferential stabilization of the ICT state with large dipole moment that becomes the lowest excited state.

Acknowledgments

The authors thank Mr. D. Pannacci for his technical assistance in HPLC measurements.

This work was supported by grants from the Ministry of Science, Education and Sports of the Republic of Croatia (grant no. 125-0982933-2926) and Ministero per l'Università e la Ricerca Scientifica e Tecnologica (Rome, Italy) and the University of Perugia [PRIN 2008, 20088NTBKR] and the Fondazione Cassa di Risparmio di Perugia (Italy).

References

[1] E. Marri, G. Galiazzo, U. Mazzucato, A. Spalletti, Chem. Phys. 312 (2005) 205–211.
[2] G. Ginocchietti, G. Galiazzo, U. Mazzucato, A. Spalletti, Photochem. Photobiol. Sci. 4 (2005) 547–553.
[3] S. Ciorba, G. Galiazzo, U. Mazzucato, M. Šindler-Kulyk, I. Škorić, A. Spalletti, J. Photochem. Photobiol. A: Chem. 187 (2007) 325–331.
[4] G. Ginocchietti, U. Mazzucato, A. Spalletti, J. Photochem. Photobiol. A: Chem. 196 (2008) 233–238.
[5] S. Ciorba, G. Bartocci, G. Galiazzo, U. Mazzucato, A. Spalletti, J. Photochem. Photobiol. A: Chem. 195 (2008) 301–306.
[6] I. Baraldi, E. Benassi, S. Ciorba, M. Šindler-Kulyk, I. Škorić, A. Spalletti, Chem. Phys. 353 (2008) 163–169.
[7] I. Baraldi, E. Benassi, A. Spalletti, Spectrochim. Acta Part A 71 (2008) 543–549.
[8] I. Baraldi, G. Ginocchietti, U. Mazzucato, A. Spalletti, Chem. Phys. 337 (2007) 168–176.
[9] S. Škorić, A. Ciorba, M. Spalletti, Šindler-Kulyk, J. Photochem. Photobiol. A: Chem. 202 (2009) 136–141.
[10] E. Baraldi, S. Benassi, M. Ciorba, I. Šindler-Kulyk, A. Škorić, Spalletti, Chem. Phys. 361 (2009) 61–67.
[11] A. Marrocchi, A. Spalletti, S. Ciorba, M. Seri, F. Elisei, A. Taticchi, J. Photochem. Photobiol. A: Chem. 211 (2010) 162–169.
[12] I. Škorić, I. Kikaš, M. Kovacs, M. Šindler-Kulyk, O. Horvath, J. Photochem. Photobiol. A: Chem. 211 (2010) 152–161.
[13] M. Šindler-Kulyk, Z. Stiplošek, B. Metelko, Croat. Chem. Acta 62 (1989) 81–87.
[14] J.B. Birks, Photophysics of Aromatic Molecules, Wiley-Interscience, London, 1970, p. 51, Eq. 3.49.
[15] G. Bartocci, F. Masetti, U. Mazzucato, A. Spalletti, I. Baraldi, F. Momicchioli, J. Phys. Chem. 91 (1987) 4733–4743.
[16] H. Görner, F. Elisei, G.G. Aloisi, J. Chem. Soc., Faraday Trans. 88 (1992) 29–34.
[17] A. Romani, F. Elisei, F. Masetti, G. Favaro, J. Chem. Soc., Faraday Trans. 88 (1992) 2147–2154.
[18] I. Carmichael, G.L. Hug, J. Phys. Chem. Ref. Data vol.15 (1986) 1–204.
[19] F. Ortica, A. Romani, G. Favaro, J. Phys. Chem. A 103 (1999) 1335–1341.
[20] R.S. Becker, G. Favaro, G. Poggi, A. Romani, J. Phys. Chem. 99 (1995) 1410–1417.
[21] L. Zechmeister, Trans–cis Isomeric Carotenoids Vitamins A and Arylpolyenes, Sprinter-Verlag, Wien, 1962.
[22] E. Marri, F. Elisei, U. Mazzucato, D. Pannacci, A. Spalletti, J. Photochem. Photobiol. A: Chem. 177 (2006) 307–313.
[23] B. Carlotti, A. Spalletti, M. Šindler-Kulyk, F. Elisei, Phys. Chem. Chem. Phys. (2011), doi:10.1039/c0cp02337j.
[24] H. Görner, F. Elisei, U. Mazzucato, G. Galiazzo, J. Photochem. Photobiol. A: Chem. 43 (1988) 139–154.